ELSEVIER

Journal of Molecular Catalysis A: Chemical 157 (2000) 151–161

JOURNAL OF MOLECULAR CATALYSIS A: CHEMICAL

www.elsevier.com/locate/molcata

Effect of zeolitic water on the carbonylation route of platinum(II) in NaX to $[Pt_3(CO)_6]_2^{2-}$ Chini complexes embedded in cavities of the zeolite

M. Beneke [a], L. Brabec [b], N. Jaeger [a], J. Nováková [b,*], G. Schulz-Ekloff [a]

[a] *Institute of Applied and Physical Chemistry of the Bremen University, FB2, Bremen University, PF 330440, D-28334 Bremen, Germany*
[b] *J. Heyrovský Institute of Physical Chemistry, Academy of Sciences of the Czech Republic, Dolejškova 3, 182 23 Prague 8, Czech Republic*

Received 6 October 1999; received in revised form 1 November 1999; accepted 11 November 1999

Abstract

The effect of water content in $[Pt(NH_3)_4]^{2+}$NaX on the direct synthesis of Pt Chini complexes $[Pt_3(CO)_6]_2^{2-}$ embedded in zeolitic cavities as well as the carbonylation process of PtNaX to the same anionic complex were studied using in situ FTIR and UV–Vis spectroscopies. It was found that the presence of water affects carbonylation route of the Pt tetrammine complexes; low water content makes this carbonylation similar to that of PtNaX. The interplay of water content and active sites needed for its decomposition via WGS reaction is assumed to play the decisive role in the reaction route. The rate of carbonylation is affected by the amount of zeolitic water, which supports migration of Pt species and supplies protons to the charge-compensating species, accelerating thus the carbonylation process. IR wavenumbers of both bridge and on-top bonded CO in platinum Chini complexes depend on the amount of water ligands. © 2000 Elsevier Science B.V. All rights reserved.

Keywords: Hydrated, dehydrated and calcined Pt tetrammine complexes; Carbonylation, WGS reaction

1. Introduction

Studies of anionic carbonyl complexes embedded in zeolites have been aimed to get (i) special catalytic properties because of the unusual redox features, and (ii) very small stable Pt clusters, containing the same number of Pt atoms as the parent anionic complex, homogeneously dispersed in the zeolite framework after the complex decomposition. The first point appeared to be matched in some reactions [1–3], the second one has often failed due to the agglomeration of the platinum clusters [3–6]. Nevertheless, some very interesting features, namely formation of platinum ''chains'' have been found [7].

To date, two routes of the ''ship-in-bottle'' synthesis of Pt Chini complexes ($[Pt_3(CO)_6]_n^{2-}$) in zeolites, predominantly faujasites, have been reported. The first one [8–15] is the direct carbonylation of the $[Pt(NH_3)_4]^{2+}$ cations by CO in the presence of small amounts of water. The

* Corresponding author.

1381-1169/00/$ - see front matter © 2000 Elsevier Science B.V. All rights reserved.
PII: S1381-1169(99)00427-6

carbonylation is assumed to proceed according to the scheme suggested in Ref. [14]:

$$3n\left[Pt(NH_3)_4\right]^{2+} + (3n+1)H_2O + (9n+1)CO \leftrightarrow \left[\{Pt_3(CO)_3(\mu\text{-}CO)_3\}_n\right]^{2-} + 2(3n+1)NH_4^+ + 2(3n-1)NH_3 + (3n+1)CO_2. \quad (1)$$

The individual steps of the carbonylation process have not been recognized yet. The second route reported in literature concerns the carbonylation of Pt^{2+} cations in zeolites by CO and traces of water [4,5,16,17], which can be expressed by the stoichiometry:

$$3nPt^{2+} + (9n+1)CO + (3n+1)H_2O \rightarrow \left[Pt_3(CO)_6\right]_n^{2-} + 2(3n+1)H^+ + (3n+1)CO_2. \quad (2)$$

Water is assumed to play the dominant role providing H atoms (consequently protons) through the WGS reaction [18].

The present paper compares direct carbonylation of Pt ammine cationic complexes in hydrated and dehydrated zeolitic matrix, and the carbonylation of Pt^{2+} cations obtained by calcination of Pt ammine cationic complex in the same zeolite. All these processes were studied in situ by UV–Vis and FTIR spectroscopies. Gaseous phase was analyzed mass spectrometrically. The assignment of various FTIR bands was supported using ^{13}CO for the carbonylation.

2. Experimental

The platinum containing NaX (3 wt.% of Pt, in some cases also 10 wt.% of Pt) were prepared by ion exchange of Na ions for $Pt(NH_3)_4^{2+}$ from corresponding dichloride and used either directly for in situ carbonylation, or decomposed in an oxygen stream at slowly increasing temperature (1°C/min) to 350°C. The calcined sample was then carbonylated in situ in the infrared cell of a Nicolet MX1E FTIR instrument. The carbonylation of Pt ammine complexes was performed using a Nicolet Protégé 460 FTIR spectrometer either in transmission mode with a DTGS detector or in diffuse reflectance mode in a Harrick cell with an MCTA nitrogen cooled detector. In the former case, self-supported wafers (7–9 mg/cm^2) were used; in the latter case small pellets (ca. 30 mg) were employed. A Cary 4 UV–Vis spectrometer equipped with a Harrick reaction chamber was employed for the carbonylation, oxidation and recarbonylation of small zeolite pellets (ca. 30 mg). Details of the samples preparation and of the measurements were described in the preceding papers [13–15,19,26]. Analysis of the gas phase during temperature programmed decomposition of carbonyls in vacuum was registered using a Balzers QMG 420 mass spectrometer.

3. Results

3.1. Carbonylation of dehydrated $Pt(NH_3)_4$NaX, FTIR spectra

The progress of carbonylation (at 90–150°C) of $Pt(NH_3)_4$NaX dehydrated in vacuum at 180°C is given in Fig. 1. Decrease of the band at 1381cm^{-1} (asymmetric bending vibrations of N–H) and 1589 cm^{-1} (symmetric bending N–H vibrations, in mildly hydrated samples hidden in water peaks) is accompanied by the increasing band at 1443 cm^{-1} (NH_4^+); formation of the anionic Chini complex $[Pt_3(CO)_6]_2^{2-}$ follows from the appearance of stretching C–O bonds of the linearly (on top) and bridged bonded CO (vibrations at 2024 and 1803 cm^{-1}, respectively). Contrary to the mildly dehydrated $Pt(NH_3)_4$NaX (at 25°C for 5–30 min) [19] an intermediate CO species vibrating at 2200 cm^{-1} appears (assigned to Pt^{2+}CO [20]), and a band at 1618 cm^{-1} is also created. While the intensity of the former band exhibits a maximum during carbonylation, that of the latter keeps

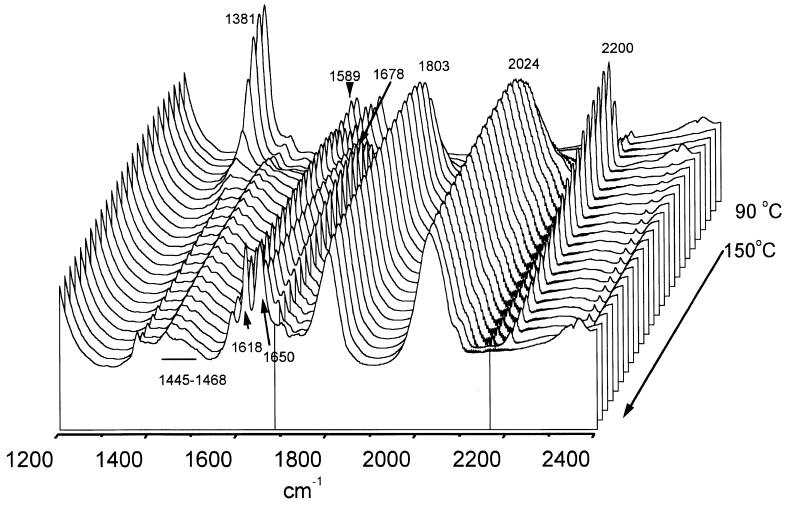

Fig. 1. FTIR spectra, carbonylation of $Pt(NH_3)_4NaX$, ^{12}CO. Sample dehydrated at 180°C, carbonylation by 600 mbar of CO, first four spectra at 90°C in 15 min intervals, then at 150°C in 30 min intervals, last spectrum after 11 h.

increasing; stability of this species is low, as it can be readily removed by oxidation at mild temperature. The band at 1678 cm^{-1} also exhibits a maximum during carbonylation.

If ^{13}CO is used for carbonylation, the bands of all species containing carbon (linear and bridge CO, Pt^{2+}–CO and the band at 1618 cm^{-1}) are shifted to lower wavenumbers [27],

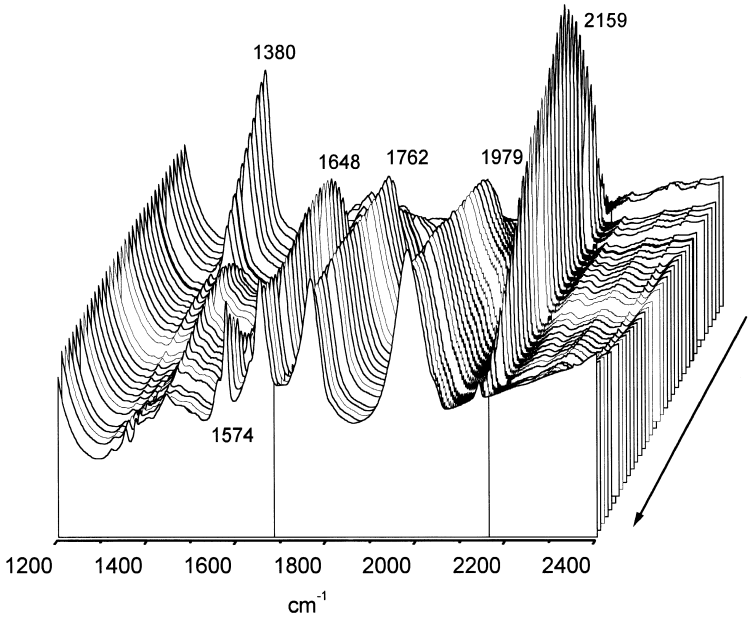

Fig. 2. FTIR spectra, carbonylation of $Pt(NH_3)_4NaX$, ^{13}CO. Sample dehydrated at 180°C, carbonylation by 500 mbar of ^{13}CO at 150°C, first 11 spectra in 10 min intervals, next 10 spectra in 20 min intervals, then in 1 h intervals.

Table 1
Position of IR bands (in cm^{-1}) during $Pt(NH_3)_4^{2+}$ and Pt^{2+} carbonylation of dehydrated samples by ^{12}CO and ^{13}CO
?[a], ?[b] some carbonates or carboxylates.

Initial Pt state + CO	Pt ammine δ_{as} N–H	NH_4^+ δ N–H	Pt ammine δ_s N–H	?[a]	H_2O δ O–H	?[b]	> C–O ν (C–O)	–C–O ν (C–O)	Pt^{2+}–CO ν (C–O)
Pt ammine + ^{12}CO	1380	1470	1587	1618	1651	–	1800	2021	2200
Pt ammine + ^{13}CO	1380	1476	–	1574	1651	–	1760	1979	2139
Pt^{2+} + ^{12}CO	–	–	–	1617	1649	1711	1797	2022	2201
Pt^{2+} + ^{13}CO	–	–	–	1574	1648	1667	1757	1976	2140
$\Delta\nu$ (^{12}CO, ^{13}CO)	–	–	–	43–4	–	44	40	42–46	61

as followed from Fig. 2 and Table 1. The shift is 40–46 cm^{-1} for all species except $Pt^{2+}CO$, in which case the difference is considerable higher (61 cm^{-1}). In some cases, especially when the sample was cooled to room temperature, the band of adsorbed CO_2 appears; the shift with ^{13}CO was in this case even higher (1345 → 1270 cm^{-1}). The latter species can be readily removed by evacuation at 25°C.

3.2. Carbonylation of Pt^{2+}NaX, FTIR spectra

The NaX zeolite with Pt ammine decomposed by calcination to Pt^{2+} species [4,17,21–26] was evacuated at 150°C for 1 h and then carbonylated at 120–180°C. The progress of carbonylation is shown in Fig. 3, spectra 2–10 (spectrum 1 stands for the initial evacuated sample). The intensity of the band at 2200

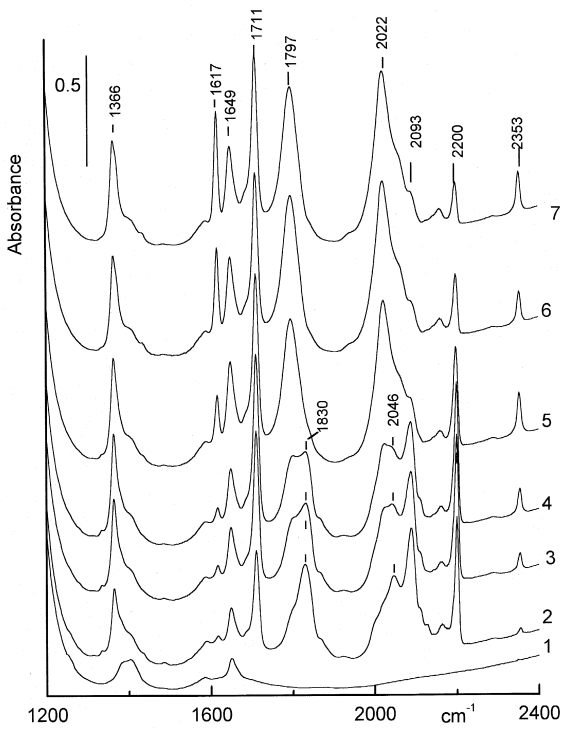

Fig. 3. FTIR spectra, carbonylation of PtNaX by ^{12}CO. Calcined $Pt(NH_3)_4$NaX to PtNaX, evacuated at 150°C for 1 h (spectrum 1), then carbonylated by 700 mbar of CO at 120°C for 1, 3 and 18 h (spectra 2–4, respectively), at 150°C for 1 and 3 h (spectra 5 and 6, respectively), at 180°C for 1 h (spectrum 7).

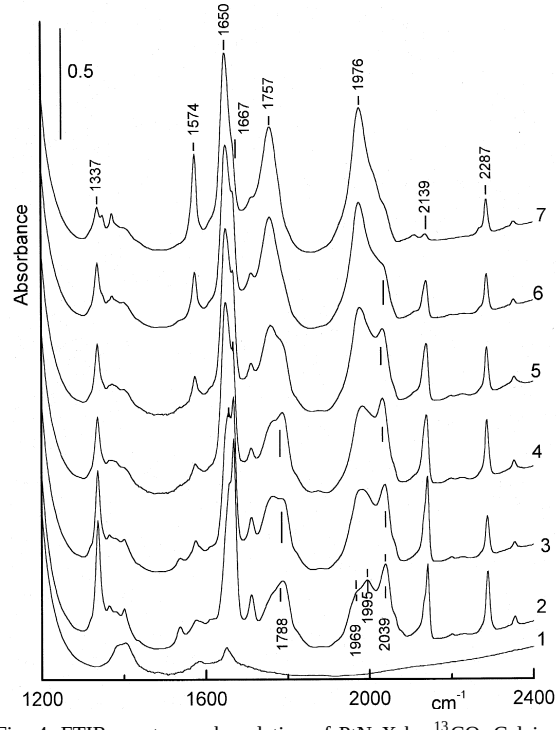

Fig. 4. FTIR spectra, carbonylation of PtNaX by ^{13}CO. Calcined $Pt(NH_3)_4$NaX to PtNaX, evacuated at 150°C for 1 h (spectrum 1), then carbonylated by 330 mbar of ^{13}CO at 120°C for 15 min and 2 h (spectra 2 and 3, respectively), then left in CO for 18 h at 25°C (spectrum 4), and carbonylation resumed at 120°C for 2, 7 and 18 h (spectra 5, 6 and 7, respectively).

cm^{-1}, which is assigned to CO adsorbed on Pt^{2+}, decreases in time, and bands of CO bridged and linearly bonded develop from the beginning additional broad and not well-resolved bands, to the bands vibrating at 1797 and 2022 cm^{-1}. In addition to bands formed during the carbonylation of Pt tetrammine, a new band vibrating at 1711 cm^{-1} is formed, the intensity of which increases in time; however, this species is only weakly bonded, as it can be removed by evacuation at 25°C. In the region of stretching OH vibrations (not shown here), the bands at 3635 cm^{-1} and those on extralattice Al (3691 cm^{-1}) are present in the spectra prior to carbonylation; the band at 3656 (HF OH) cm^{-1} and a broad one at 3585 (LF OH) cm^{-1} are formed during the carbonylation. The calcination of Pt tetrammine NaX to PtNaX prior to carbonylation removed all the N–H species.

The same procedure of Pt^{2+} carbonylation in NaX zeolite was performed using ^{13}CO. The spectra are displayed in Fig. 4. Shifts to lower wavenumbers due to the ^{13}C labeling concern, similarly to ammine carbonylation, linearly and bridged bonded CO, and CO on Pt^{2+} (Table 1). The band at 1711 cm^{-1} is shifted to 1667 cm^{-1}, and therefore this species, not present in the carbonylation of Pt tetrammine, also contains carbon.

The course of PtNaX carbonylation exhibits similar features as the recarbonylation of the oxidized carbonyl [19], i.e., narrowing of both main CO bands with progressing carbonylation. However, the recarbonylation of the oxidized

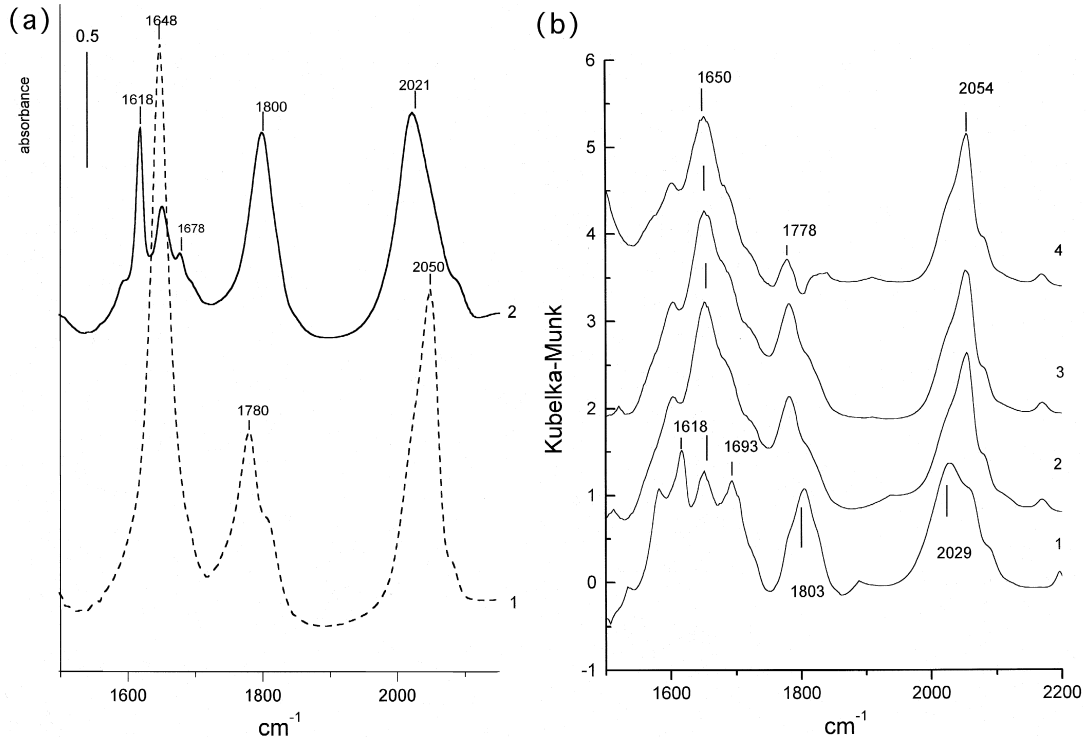

Fig. 5. Effect of water vapour on the position of FTIR bands of $[Pt_3(CO)_6]_2^{2-}$ $NaNH_4X$ (diffuse reflectance spectra). (a) Spectra 1 and 2 — carbonyls on weakly and strongly dehydrated $Pt(NH_3)_4NaX$, and (b) effect of addition of water vapours on the spectrum of Pt carbonyl prepared on strongly dehydrated $Pt(NH_3)_4NaX$; spectrum 1 — initial carbonyl; spectra 2, 3 and 4 — after 15 min interaction with 1, 2 and 3 mbar of water vapours, respectively.

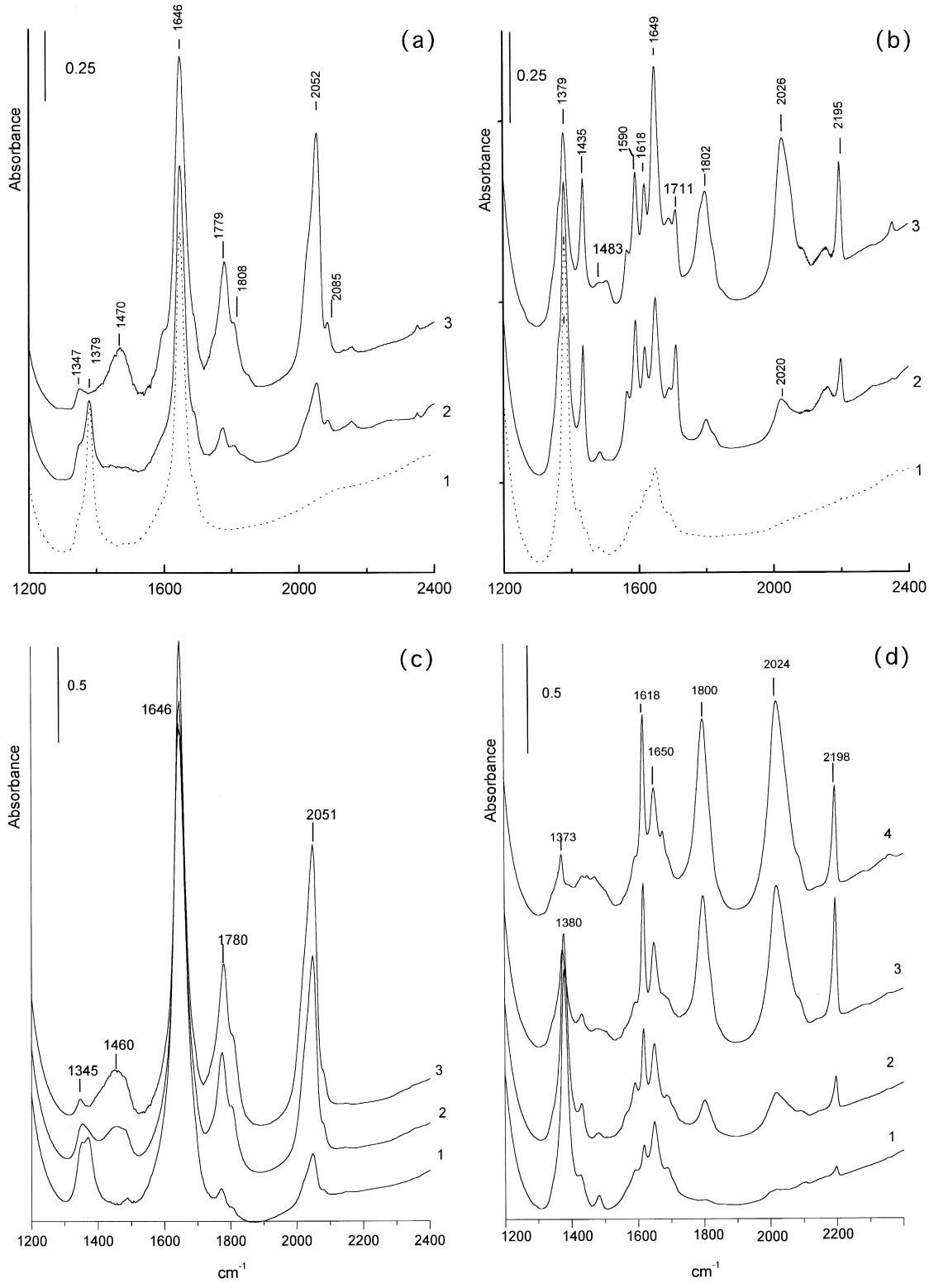
(a)
0.25
Absorbance
1646
2052
1779
1808
2085
1470
1347
1379
3
2
1
1200
1600
2000
2400
(b)
0.25
Absorbance
1379
1649
1435
1590
1618
1711
1802
2026
2195
1483
2020
3
2
1
1200
1600
2000
2400
(c)
0.5
Absorbance
1646
2051
1780
1460
1345
3
2
1
1200
1400
1600
1800
2000
2200
2400
cm-1
(d)
0.5
Absorbance
2024
1618
1800
1650
2198
1373
1380
4
3
2
1
1200
1400
1600
1800
2000
2200
cm-1

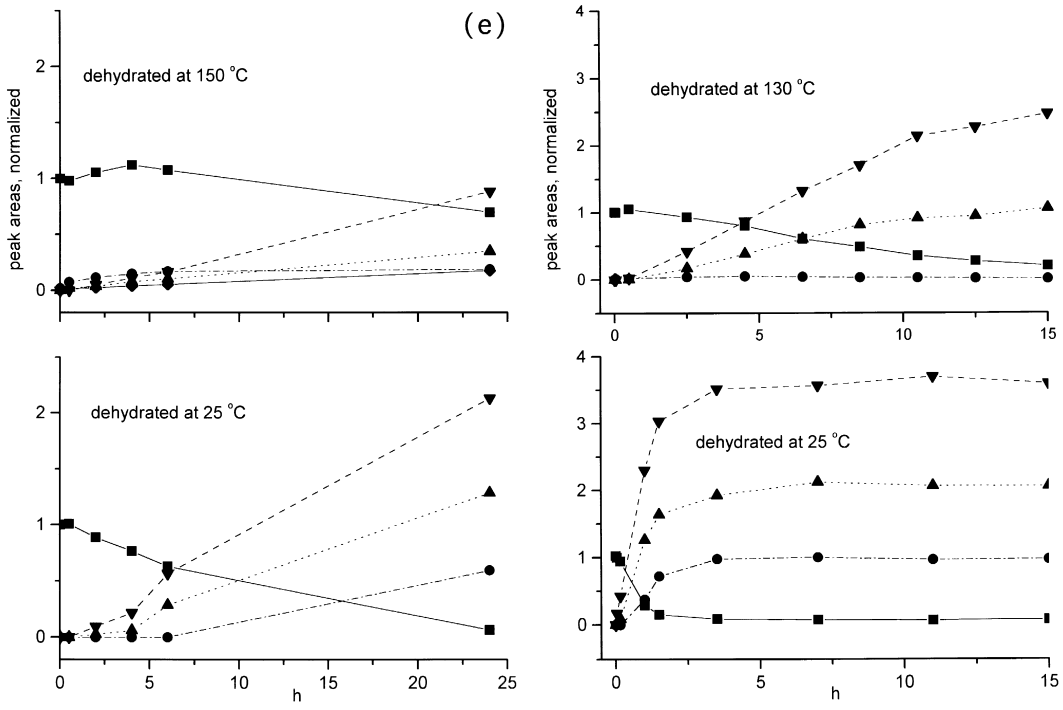

Fig. 6. Effect of dehydration temperature on the course of carbonylation, FTIR spectra. (a and b) Samples dehydrated at 25°C (30 min) and 150°C (2 h), respectively. Both (a) and (b) samples carbonylated at 90°C by 600 mbar of CO: spectra 1, dotted — before carbonylation; spectra 2 and 3 — after carbonylation for 6 and 15 h, respectively. (c and d) Samples dehydrated at 25°C (10 min) and 127°C (0.5 h), respectively. Both (c) and (d) samples carbonylated at 127°C by 600 mbar of CO. (c) Spectra 1, 2 and 3 — after carbonylation for 10 min, 1 h and 15 h, respectively. (d) spectra 1, 2, 3 and 4 — after carbonylation for 0.5, 3, 9 and 15 h, respectively. (e) Time dependence of the integrated areas, normalized to the original N–H band (1380 cm^{-1}, squares, full line); NH_4^+ bands — circles, dash-dotted; bridge bonded CO — up triangles, dotted; linearly bonded CO — down triangles, dashed; bottom part — mildly dehydrated sample, top part — strongly dehydrated sample; left-hand side — carbonylation at 90°C, right hand side — carbonylation at 130°C.

carbonyl proceeds very rapidly and Pt^{2+}–CO bonds are not created.

3.3. Effect of zeolite dehydration on the position of CO ligands in Pt Chini complexes and on the rate of carbonylation, FTIR spectra

If the zeolite is prior to carbonylation dehydrated in vacuum only at 25°C (removal of zeolitic water from 20% to 60% in dependence on evacuation time), the resulting Pt Chini complex exhibits IR bands at 2053 and 1779 cm^{-1} for linearly and bridged bonded CO, respectively. This is compared in Fig. 5a with the positions of CO ligands in strongly dehydrated samples (spectra 2 vs. 1): the bridged bonded CO is shifted to higher value by ca. 20 cm^{-1}, while the linearly bonded CO exhibits an opposite shift. The same effect is exhibited when water vapours are added to the anionic Pt carbonyl formed on previously dehydrated sample, as is shown in Fig. 5b: spectra 2–4 correspond to the 5 min interaction with 1, 2 and 3.5 mbar of H_2O, respectively.

Fig. 6a–d shows the effect of $Pt(NH_3)_4NaX$ dehydration prior to carbonylation on the rate of carbonylation: (a) and (b) display the carbonylation at 90°C of the mildly and strongly dehydrated parent sample, respectively; (c) and (d) show the carbonylation at 127°C again of the mildly and strongly dehydrated samples. It follows that in both cases, the carbonylation proceeds more rapidly on weakly dehydrated samples, which is summarized in Fig. 6e. Here, the

integrated values of the individual bands (normalized to the parent Pt tetrammine band at 1380 cm^{-1}) are given for the mildly and strongly dehydrated samples (bottom and top lines, respectively), carbonylated at 90°C (left-hand side) and 130°C (right-hand side).

The band assigned to Pt^{2+}–CO (at 2200 cm^{-1}), as well as that at 1618 cm^{-1}, is formed only on strongly dehydrated samples regardless of the carbonylation temperature.

3.4. Carbonylation of $Pt(NH_3)_4$NaX, effect of water content, UV–Vis spectra

The UV–Vis spectra of the Pt Chini complex formed on PtNaX dehydrated at three different temperatures (60°C, 120°C and 180°C for 15 min, respectively) and carbonylated at 180°C for 90 min, are shown in Fig. 7. A shift to higher wavelenghts with increasing dehydration is clearly visible.

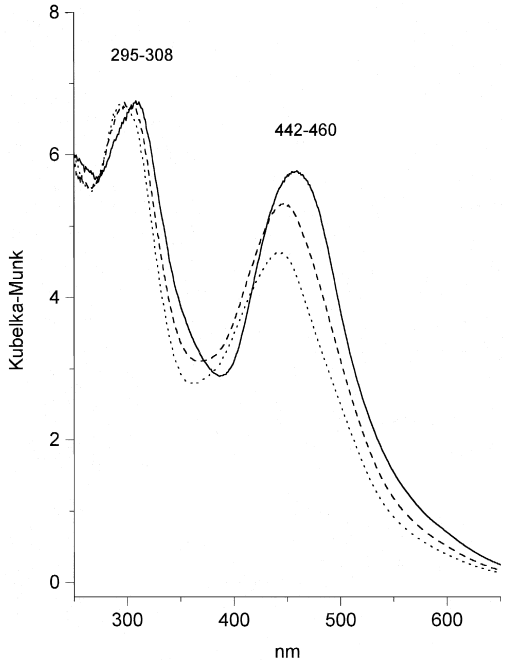

Fig. 7. Effect of the dehydration temperature on the UV–Vis spectra of $[Pt_3(CO)_6]_2^{2-}$ $NaNH_4X$. Carbonylation by 1200 mbar of CO at 180°C for 90 min; dotted, dashed and full-line spectrum — after dehydration at 60°C, 120°C and 180°C, respectively.

4. Discussion

It was mentioned in the Introduction section, that the ship-in-bottle synthesis of platinum Chini complexes in the cavities of zeolites can be achieved either by direct carbonylation of $[Pt(NH_3)_4]^{2+}$ or by carbonylation of Pt^{2+}, which both compensate together with alkali cations the negative charge of zeolitic oxygens. When anionic Chini complexes are formed, their charge must be compensated: NH_4^+ ions play this role in the former case according to Eq. 1 (confirmed by the appearance of the respective band in IR spectra at about 1450 cm^{-1}), and in the latter case, protons (from traces of water) substitute bare (stripped off of the ammine ligand) Pt^{2+} (Eq. 2). This has led to the assumption that the reductive carbonylation proceeds via hydrogen created by the WGS reaction [18]: $CO + H_2O \rightarrow CO_2 + 2H$; protons formed from the H atoms equilibrate the charge of the zeolitic oxygens either in the form of ammonium ions or framework OH groups. Active sites enabling the WGS reaction have not been specified. Presence of water — usually reported as ''traces of water'' — is thus the necessary condition enabling reductive carbonylation to anionic carbonyl complexes. The second condition, well known from the synthesis of Chini complexes in solutions, is the alkaline environment [4,12,28–30]. This is provided by alkali ions in zeolites; the ability to form Chini complexes was found to increase with the increasing basicity of zeolitic oxygen in order of alkali cations: Li < Na < K (< Cs) [13,14]. In the following, the attention will be paid to the effect of water vapours and to the possible role of Pt^{2+} cations on the route of carbonylation.

4.1. Effect of the amount of zeolitic water on the formation of Pt anionic carbonyl complexes in NaX

Pt tetrammine complexes are supposed to be homogeneously dispersed in zeolitic large cavi-

ties; for the 3 wt.% Pt load, every third cavity in average contains one ammine complex, i.e., the formation of $[Pt_3(CO)_6]_2^{2-}$ needs a powerful migration of Pt species. This transport is most probably enabled by the zeolitic water and therefore formation of the Pt Chini complexes occurs with higher rate in hydrated samples, regardless of the carbonylation temperature (naturally below that of carbonyl decomposition), as is documented in Fig. 6a–d. In Fig. 6e, the integrals of the individual bands, related to the original N–H band in Pt ammine complex, are displayed. A substantially higher carbonylation rate of mildly dehydrated samples is evident. It is worth mentioning that the higher Pt load (10 wt.%) results in a substantially higher carbonylation rate, most probably by the increased vicinity of Pt, favoring the migration–aggregation process. Higher amount of zeolitic water also contributes to the WGS reaction, thus accelerating the process.

There appeared a marked difference in the carbonylation of mildly and strongly dehydrated Pt tetrammine complex: in the latter case, the intermediate formation of the IR band vibrating at 2200 cm^{-1} (2159 cm^{-1} with ^{13}CO) was found, which we assigned to Pt^{2+}–CO. This assignment was made according to Ref. [20] and in line with the same band formed during the carbonylation of PtNaX. It seems that in the absence of ''sufficient'' amount of zeolitic water the carbonylation can proceed via the Pt^{2+} stripped off of the ammine ligands. However, it is not possible to exclude that the same mechanism occurs in hydrated samples in which the carbonylation of the ''bare'' Pt^{2+} (Pt^{2+} with H_2O ligands?) is so rapid that it could not be recorded. No intermediate NH_3–Pt–CO bonds were found pointing to a stepwise carbonylation mechanism. Drozdová and Kubelková [15] reported on the same rate of the Pt tetrammine removal and Pt Chini complex formation in faujasites, the finding of which, however, can support both the rapid carbonylation of ''bare'' Pt^{2+} and/or short-living Pt–ammine–carbonyl intermediates. The appearance of Pt^{2+}–CO intermediate species found during the carbonylation of the dehydrated Pt tetrammine NaX can naturally be only a simultaneously proceeding carbonylation route and not necessarily the only carbonylation intermediate.

The carbonylation of dehydrated Pt ammine complexes results not only in the creation of Pt Chini complexes, but simultaneously some relatively weakly bonded carboxylates or carbonates are formed (the band at 1618 cm^{-1}, and in PtNaX carbonylation also a band at 1711 cm^{-1}). The Pt^{2+} species could be assumed as active sites activating water and CO for the WGS reaction (partial CO dissociation is assumed in Ref. [19], based on the carbon deposit laid in the zeolite during carbonylation). The fact that during the recarbonylation of the oxidized carbonyls, the intermediate formation of Pt^{2+}–CO species was not observed, supports the assumption given in Ref. [19] that mild oxidation preserves in some way the arrangement of Pt atoms characteristic for the Chini complex. The possible changes in nuclearity of Pt Chini complexes due to redox processes will be discussed in the following paper.

4.2. Effect of the water amount on the position of IR and UV–Vis bands of CO in Pt Chini complexes

The position of the linearly, as well as bridged bonded CO in IR spectra, is reversibly dependent on the presence of water vapours. It is therefore tempting to assume that water ligands participate in these shifts. Similar effects were reported for $Rh^+(CO)_2$ complexes in zeolites [31]: the stretching Rh–CO frequencies for $Rh^+(CO)_2(O_{zeol})_2$ were found at 2099 and 2021 cm^{-1}, for $Rh^+(CO)_2(O_{zeol})(H_2O)$ at 2117 and 2050 cm^{-1}. In our case, the linear CO bonds in hydrated Pt Chini complex also occur at higher frequency (e.g., Fig. 5a and b, the difference is of about 30 cm^{-1}). The opposite shift is, however, obtained for the bridging CO, where the frequency in hydrated sample is by ca. 20 cm^{-1} lower than that in dehydrated sample. The linear

Pt–CO are assumed to be oriented to the zeolitic oxygens [13,14]. A lower frequency of the C–O bond in CO linearly bonded can agree with the stronger interaction of $C–O–O_{zeol}$ in the absence of water, and thus with a weakening of the C–O bond. The Chini complex can be slightly deformed due to this interaction, which can result in the opposite shift in the bridge-bonded CO. The shifts of the IR frequencies do not seem to be related to the changes in the nuclearity of Pt Chini complexes: the increased nuclearity results in the shifts of both linearly and bridged CO ligands to higher wavenumbers (e.g., Ref. [7]).

Shifts of the maxima to higher wavelengths with increasing dehydration temperature found in the UV–Vis spectra (Fig. 7, shifts 13 and 18 nm, corresponding to 0.18–0.11 eV, respectively) can be due to a lower stability of the ground electronic state of the complex in dehydrated state.

5. Conclusions

(i) The carbonylation of the dehydrated Pt tetrammine complex in NaX zeolite is accompanied by the intermediate formation of Pt^{2+}–CO species, which disappear after removal of all the Pt tetrammine ions by the reaction. The same species are temporarily formed during the carbonylation of PtNaX zeolite and can thus serve as an intermediate of the formation of Pt Chini complex. This reaction route could also proceed during the carbonylation of hydrated zeolite, but in such case it should be very rapid because no Pt^{2+}–CO species were found in this case. Another process, a stepwise substitution of ammine ligands by CO cannot be excluded, however, such intermediate species were not detected.

(ii) Zeolitic water present in hydrated samples helps in the migration of Pt species and adds protons to the charge equilibration accelerating thus the carbonylation process.

(iii)The IR band of on-top bonded CO in carbonyls is shifted to lower frequency in dehydrated sample compared to the zeolite in hydrated form while the opposite is found for the bridged bonded CO. This is ascribed to the participation of water ligands in hydrated samples.

Acknowledgements

This study was supported by the Grant Agency of the Academy of Sciences of the Czech Republic (A4040710) and the Deutsche Forschungsgemeinschaft (436TSE 113/30/0).

References

[1] G.J. Li, T. Fujimoto, A. Fukuoka, M. Ichikawa, New frontiers in catalysis, in: L. Guczi (Ed.), Int. Congr. Catal., 10th, 1992, Elsevier, 1993, p. 1607.
[2] H.H. Lamb et al., Catal. Today 18 (1993) 3.
[3] M. Ichikawa, T. Yamamato, W. Pan, T. Shido, Progress in zeolite and microporous materials, Stud. Surf. Sci. Catal. 105 (1997) 679.
[4] B.C. Gates, Chem. Rev. 95 (1995) 511.
[5] M. Ichikawa, in: K. Tamaru (Ed.), Dynamic Processes on Solid Surfaces, Plenum, New York, 1993, p. 149.
[6] R. Ugo, C. Dossi, R. Psaro, J. Mol. Catal. A: Chem. 107 (1996) 13.
[7] M. Sasaki, M. Osada, N. Higashimoto, T. Yamamoto, A. Fukuoka, M. Ichikawa, J. Mol. Catal. A: Chem. 141 (1999) 223.
[8] M. Ichikawa, J. Chem. Soc., Chem. Commun. (1976) 11.
[9] M. Ichikawa, Chem. Lett. (1976) 335.
[10] A. De Mallmann, D. Barthomeuf, Catal. Lett. 5 (1990) 213.
[11] Y. Yokomichi, T. Nakyama, O. Okada, Y. Yokoi, I. Takahashi, H. Uchida, H. Ishikawa, R. Yamaguchi, H. Matsui, T. Yamabe, Catal. Today 29 (1996) 155.
[12] M. Ichikawa, in: K. Tamaru (Ed.), Dynamic Processes on Solid Surfaces, Plenum, New York, 1993, p. 149.
[13] L. Kubelková, J. Vylita, L. Brabec, L. Drozdová, T. Bolom, J. Nováková, G. Schulz-Ekloff, N.I. Jaeger, J. Chem. Soc., Faraday Trans. 1 92 (1996) 2035.
[14] L. Kubelková, L. Drozdová, L. Brabec, J. Nováková, J. Kotrla, P. Hülstede, N.I. Jaeger, G. Schulz-Ekloff, J. Phys. Chem. 100 (1996) 15517.
[15] L. Drozdová, L. Kubelková, J. Chem. Soc., Faraday Trans. 93 (1997) 2597.
[16] T. Yamamoto, T. Shido, S. Inagaki, Y. Fukushima, M. Ichikawa, J. Phys. Chem. B 102 (1998) 3886.
[17] W.M.H. Sachtler, Z. Zhang, Adv. Catal. 39 (1993) 129.
[18] H. Bischoff, N.I. Jaeger, G. Schulz-Ekloff, L. Kubelková, J. Mol. Catal. 80 (1993) 95.
[19] Z. Bastl et al., in preparation.

[20] G. Schulz-Ekloff, R. Lipski, N.I. Jaeger, P. Hülstede, L. Kubelková, Catal. Lett. 30 (1995) 65.
[21] N. Jaeger, A.L. Jourdan, G. Schulz-Ekloff, J. Chem. Soc., Faraday Trans. 87 (1991) 1251.
[22] P. Gallezot, Catal. Rev.-Sci. Eng. 20 (1979) 122.
[23] R. Ryoo, S.J. Cho, Ch. Pak, Catal. Lett. 20 (1993) 107.
[24] M.S. Tzou, B.K. Teo, W.M.H. Sachtler, J. Catal. 113 (1988) 220.
[25] A.C.M. Van den Broek, J. van Grondell, R.A. van Santen, J. Catal. 167 (1997) 417.
[26] J. Nováková, L. Brabec, J. Catal. 166 (1997) 186.
[27] S. Pinchas, I. Laulicht, in: Infrared Spectra of Labelled Compounds, Academic Press, New York, 1971, p. 242.
[28] J.C. Calabrese, F.D. Dahl, P. Chini, G. Longoni, S.J. Martinengo, J. Am. Chem. Soc. 96 (1974) 2614.
[29] G. Longoni, P. Chini, J. Am. Chem. Soc. 98 (1976) 7225.
[30] B.E. Handy, J.A. Dumesic, S.H. Langer, J. Catal. 73 (1990) 126.
[31] T.T. Wong, A.Yu. Stakheev, W.M.H. Sachtler, J. Phys. Chem. 96 (1992) 7733.